Impacts of Raindrops Increase Particle Sedimentation in a Sheet Flow

Amina Nouhou-Bako[1,2], Lionel Cottenot[1], Pierre Courtemanche[1], Carine Lucas[2], François James[2], Frédéric Darboux[1,3†]

[1] URSOLS, INRAE, 45075 Orléans, France.

[2] Institut Denis Poisson, Université d'Orléans, Université de Tours, CNRS UMR 7013, Route de Chartres, BP 6759, 45067 Orléans cedex 2, France.

[3] Université de Lorraine, INRAE, LSE, 54000 Nancy, France.

†Current address: ETNA research unit – INRAE, Domaine Universitaire, BP 76, F-38402 Saint-Martin-d'Hères cedex, France.

Corresponding author: Frédéric Darboux, Frederic.Darboux@inrae.fr

Author contributions

Amina Nouhou-Bako	a, c, d, e, h
Lionel Cottenot	c, d, i
Pierre Courtemanche	c, d
Carine Lucas	a, b, c, g, h, i
François James	a, b, c, g, i
Frédéric Darboux	a, b, c, d, e, g, h, i

(a) conceptualization; (b) funding acquisition; (c) methodology (including methodological development); (d) investigation (e.g. data collection); (e) resources (provision of data etc); (f) software (its provision and development); (g) supervision; (h) writing – initial draft; and (i) writing – reviewing and editing.

Acknowledgments

The authors thank the Région Centre-Val de Loire and INRAE for the PhD fellowship of Amina Nouhou-Bako. The project “Multiparticular transfer by overland flow” of CNRS-INSU 2016 TelluS-INSMI-MI funded part of the experiments. The authors would also like to thank the two anonymous reviewers for their constructive feedback that was of great help in improving the manuscript.

Data Availability Statement

Data archiving is under way at https://data.inrae.fr.

Impacts of Raindrops Increase Particle Sedimentation in a Sheet Flow

Abstract

Interrill erosion is driven by raindrops and sheet flow. Raindrop impacts cause sediment detachment and splash, but can also affect flow transport. Even if these processes have been studied for long, the actual effect of raindrop impacts on particle settling velocities has not been experimentally assessed. This leads to unconstrained adjustments in the soil erosion models, the settling velocity of particles being a freely adjustable parameter allowing for better fitting the particle flux measured at the outlet. To address the effect of raindrop impacts on the settling of particles in sheet flow, a laboratory flume experiment was designed, using an upstream feeder of sediment (100–200 µm) and simulated rainfalls. It reproduced conditions close to sheet flow, while not allowing for the detachment of particles from the flume bottom. Two series of experiments were run: a series with a high rainfall intensity (175 mm h^{-1}) generated by an oscillating-nozzle rainfall simulator, and a series with lower rainfall intensities (10, 15, 25, 35, 55 mm h^{-1}) generated by a drop-former rainfall simulator. When a rainfall was applied, it systematically decreased the sediment concentration at the outflow compared to the no rain condition, however no obvious relationship was found with the rainfall intensity. This shows that raindrop impacts increase particle settling velocities in sheet flow. Two underlying mechanisms are suggested, related to the momentum of the raindrops or to the turbulence caused by the raindrops into the flow. Further studies should be carried out, using computational fluid dynamics and collaboration with the fluid mechanics community.

Keywords: Rainfall, sediment flux, overland flow, interrill, settling velocity

1 Introduction

In interrill areas, raindrop impacts and sheet flow are the main soil erosion drivers. If their respective role and their interactions has driven many research works, it remains a subject of debate (Kinnell, 2005; Zhang, 2019). Numerous works have shown that the impacts of raindrops are a major contributor to sediment detachment for sheet flow (Moss and Green, 1983; Moss, 1988; Proffitt and Rose, 1991). While raindrop impacts detach soil particles and move them in a range of a few decimeters at most by splash (Ghadiri and Payne, 1988; Leguédois et al., 2005), the sheet flow — a shallow and slow movement of water at the soil surface — is able to transfer them downslope (Kinnell, 1990, 2005). When sheet flow is present, raindrops can also affect flow transport, which has been termed “raindrop-induced flow transport” (or RIFT) (Kinnell, 2005). RIFT has been shown to be more efficient than splash to move particles from interrill areas to rills (Kinnell, 2005). Raindrop impacts are the most effective in detaching soil particles when water depth is between two and three raindrop diameters (Moss and Green, 1983; Kinnell, 1991). For larger flow depth, the water layer protects the soil from the raindrop impact, while, for smaller flow depth, the raindrop-induced shear stress has a shorter duration and limited spatial extend (Nouhou-Bako et al., 2019). From a physical point-of-view, Kinnell (2021) states that the distance traveled by coarse particle depends (1) on the height to which the particle are lifted, (2) on the velocity of the flow, and (3) on the settling velocity of the particles. However, the effect of raindrops on the settling velocity is not specified.

The interactions between raindrops, sheet flow, and sediments, have fostered many studies about interrill erosion, and have allowed for the design of process-based soil erosion models. The Hairsine and Rose model (Hairsine et al., 2002) includes five processes affecting particle fate: four processes for erosion (rainfall detachment, rainfall redetachment, entrainment and reentrainment) and one process for deposition (simply termed deposition). Because the transfer of particles is based on the mass-balance between these five processes, the overall particle output of the model is very sensitive to the proper parametrization of the single deposition process. As defined by Hairsine et al. (2002), this deposition process depends on the sediment concentration (with a possible vertical gradient) and on the particle settling velocity. This means the settling velocity is a key parameter of the whole modeling effort. In the transport-distance approach of Wainwright et al. (2008), the model accounts for three detachment conditions and four transport modes. While sediments are divided into size classes (to allow for selective transport) with specific settling velocities, Wainwright et al. (2008) do not give insights about the definition or measurement of these settling velocities. Similar observations are made for the models LISEM (De Roo et al., 1996) and EUROSEM (Morgan et al., 1998).

Currently, no measurements are available for settling velocities in raindrop-impacted flows. This questions our ability to properly parametrize the Hairsine and Rose model for such flows: Do particles in a rain-impacted flow settle with the same velocity as in still-water? Currently, applications of Hairsine and Rose model take still-water settling velocities as a reference, and can adjust them to get a better fit of their calibration dataset. Tromp-van Meerveld et al. (2008) decreased the settling velocities of particles larger than 315 µm, suggesting raindrop impacts slow down their sedimentation, but increased the settling velocities of particles smaller than 315 µm, suggesting raindrop impacts accelerate their sedimentation. Jomaa et al. (2010) increased the settling velocities for the whole range of particle classes (lower than 2 µm to larger than 1000 µm) for two of their experiments, suggesting raindrop impacts accelerate the sedimentation for all particles. For two other experiments, Jomaa et al. (2010) kept the still-water settling velocities for all particle sizes except for the 100–1000 µm range for which the settling velocity was decreased, suggesting raindrop impacts have a selective effect on the sedimentation. Nord and Esteves (2005) kept the settling velocities equal to the still-water settling velocities, suggesting raindrop impacts have no effect on sedimentation. While these discrepancies may be related to the actual processes occurring in the flow, it must be noted that there is no experimental data evaluating the effect of raindrops on particles transported by sheet flow. Hence, settling velocity is used as an adjustable parameter.

While the effect of raindrop impacts on particle detachment and splash has been well-documented, the actual effect of raindrop impacts on particle sedimentation is completely unknown. In fact, experimental studies did not measure detachment and sedimentation separately: they measured the mass balance of these two opposite processes at the outlet (Moss, 1988; Proffitt et al., 1991; Huang, 1995; Römkens et al., 2002; Kuhn and Bryan, 2004; Kinnell, 2011). Hence, the specific effect of raindrop impacts on sedimentation is undefined. While constraints on the settling velocities in raindrop-impacted flows could be prescribed in soil erosion models, there is no available data.

The two goals of the present paper are (1) to ascertain that particle settling is affected by raindrop impact in a sheet flow and (2) to quantify this effect depending on rainfall intensity. A dedicated experiment, making use of a laboratory flume under rainfall simulation, was carried out. One of the challenges was to study only one process: the interaction between the raindrop impacts and the particles transported and settling in the flow. As a consequence, an experimental setup was specifically designed to avoid (1) particle (re-)detachment and (2) particle-to-particle interactions (such as (dis-)aggregation), while keeping experimental conditions resembling sheet flow.

2 Materials and Methods

The experimental setup described below allowed for the assessment of the effect of raindrop impacts on particle sedimentation. It makes use of a flume, a particle feeder and two rainfall simulators (in two sets of runs). Rainfall simulators permitted a good control of the experimental conditions and facilitate replication. Rainfall intensity, water depth, water velocity, water flux were measured to assess the hydrodynamic properties. Particle concentration at the outlet was measured to assess the effect of raindrop impacts on particle fate.

A first set of experiments, using an oscillating-nozzle rainfall simulator, was run at a very high rainfall intensity to maximize the potential interaction between raindrop impacts and flow-transported particles, and hence answer the first goal. A second set of experiments made use of a drop-former rainfall simulator and was run with lower rainfall intensities to characterize the particle-raindrop interaction, tackling the second goal.

2.1 Flume

The flume had a length of 1.9 m, a width of 50 cm and a height of 15 cm (Figure 1). It was set horizontal. Conceptually, the flume consisted of four sections, which were, from upstream to downstream: a water supply and stabilization section (98 cm long), a particle-supply section (9 cm long), an experimental section (53 cm long) and an outlet section (30 cm long).

Except for the outlet section, the flume had a rough bottom made with glued sand grains (between 1 and 2 mm in diameter). This was designed to trap sedimented particles and to avoid their subsequent detachment.

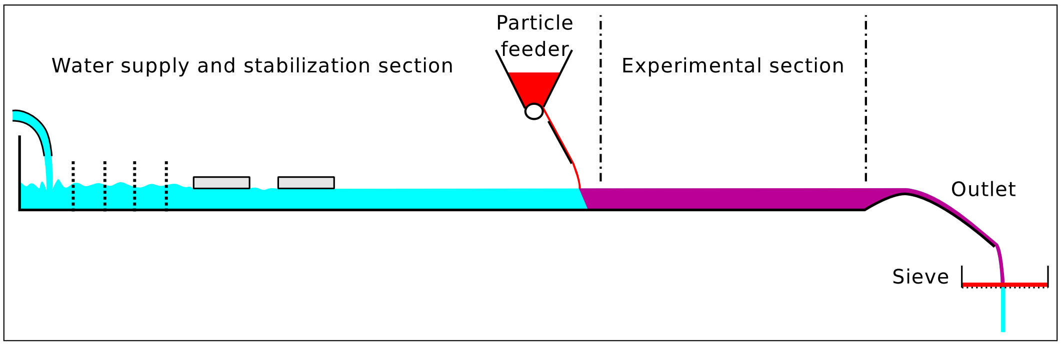

Figure 1: Scheme of the experimental setup. The water flow is supplied at the upstream end of the stabilization section. The particles are fed at the end of this section. Then follows the experimental section (only section with rainfall) and the outlet section. The particles reaching the outlet are collected in a sieve.

The water inflow consisted of a horizontal pipe inserted, at the upstream boundary of the flume, perpendicularly to the flow direction. The pipe contained holes regularly distributed over its length. The inflow rate (about 73 L min^{-1}) could be adjusted with a vane. The water flow was stabilized with scouring pads, wire meshes and floats spread along the upper 50 cm of the flume. This created a sub-critical (Froude number: 0.2), laminar (Reynolds number: 2250), and homogeneous flow. In the absence of rain, no wave was visible at the water surface.

A particle feeder was located 9 cm upstream from the experimental area in order to protect it from water splash. It was designed to provide an homogeneous distribution over the width of the flume. The particle feeder consisted of a hopper (containing the stock of particles) standing on a roller wrapped in 200 µm-particle-size emery cloth to ensure particle racking. The roller rotation was controlled by a step-by-step motor used in micro-stepping mode. The rotational speed was set to 1.36 round min^{-1}, giving a particle supply rate of 0.23 ± 0.02 g min^{-1} cm^{-1} along the flume width. This rate of particle supply was chosen to get a very low particle concentration (about 0.15 g L^{-1}), which should help in limiting the particle-to-particle interactions. A powder of clay brick was found appropriate in avoiding (dis)aggregation processes. The particle bulk density was 2.3 g cm^{-3}, and the particle size was between 100–200 µm, leading to settling velocities of 5–16 mm s^{-1} based on Cheng (1997). The particles slid on a metal sheet before reaching the water. One of the design criteria of the experiment was that no particle (re-)detachment occurred. Preliminary testing confirmed this: after reaching the bottom of the flume, the particles did not move further downstream for the whole range of experimental conditions (water flux, rainfall intensity, etc.).

Rainfall was applied only in the experimental section, the other sections having roofs and vertical screens. Roofs and vertical screens were covered with geotextile to avoid that rain water splashed in the experimental area. The outlet section was fitted with an adjustable weir that allowed for adjusting the water depth. The weir geometry created a supercritical flow at the outlet, preventing any upstream-moving wave to perturb the flow in the experimental section of the flume.

2.2 Rainfall simulators

Two types of rainfall simulators were successively used in two separated series of experimental runs.

The oscillating-nozzle rainfall simulator used the same design as the one described in Foster et al. (1979). Two troughs were used, located 6.5 m above the flume. Each trough was equipped with two nozzles (65100 Vee-jet, Spraying Systems Co.), and the water pressure in the ramps was set to 0.8 bar, leading to a prescribed rainfall intensity of 175 mm h^{-1}. Since this prescribed value may not correspond to the actual rainfall intensity, rainfall intensity will be measured (see below). This extremely high rainfall intensity was intended to maximize the interactions between settling particles and raindrops. The mean drop diameter of the rainfall, measured with a spectro-pluviometer (Laser Precipitation Monitor, Thies Clima), was 1.7 mm, with a velocity of 5.8 m s^{-1}. The kinetic energy of the rainfall was 7 J m^{-2} mm^{-1}. By design, the rainfall was discontinuous in time: oscillating-nozzle rainfall simulators generate a succession of raindrop pulses. To minimize this inconvenience, the two troughs were set to oscillate alternatively at an individual rate of 100 pulses per minute, leading to a pulse every 0.3 s. Since this periodic sequence of rain and no-rain time intervals (even if very short) may affect the particle transfer processes, supplementary experiments were carried out with a drop-former rainfall simulator. This was also the opportunity to test for the effect of rainfall intensity.

The drop-former rainfall simulator (Cottenot et al., 2021) was designed to give a rainfall both homogeneous in space and continuous in time, at lower rainfall intensities than the oscillating-nozzle simulator. It was made with porous pipes of 16 mm in diameter. The pipes were aligned horizontally and separated by 24 mm. They were attached on a grid every 20 mm with tie straps. Drops formed preferentially at the tie straps. The pipes were supplied in water by a manifold. A manometer, fixed on the manifold, allowed to set the water pressure. A mesh with square openings of 3 mm was attached 65 cm below the pipes to break the drops and to allow for a higher spatial homogeneity. The mesh of the simulator was located at 6.6 m above the flume. The frame supporting the whole simulator was slightly and continuously moved horizontally to improve further the spatial homogeneity. The spectropluviometer gave a mean raindrop diameter of 3.0 mm with a velocity of 7 m s^{-1}, and a kinetic energy of about 20 J m^{-2} mm^{-1}. Raindrop characteristics were independent of the water pressure. The simulator was used with pressures ranging from 0.18 to 1.4 bar, leading to prescribed intensities from 10 to 55 mm h^{-1} (the actual rainfall intensity will be measured — see below). The Christiansen's uniformity coefficient of the rainfall intensity was always above 90 %.

2.3 Measurements

At the beginning of each experimental run, rainfall intensity was measured within the experimental section by timing the partial filling of 28 cylindrical beakers (64 mm in diameter) and weighing their content. It was used to check the proper setup of the rainfall simulator. During the actual experimental rain, rainfall intensity was checked using four or eight beakers.

In the absence of rainfall, the water depth was measured as the difference between the height of the water surface and the height of the flume bottom using a mechanical comparator. During the rainfall application, no accurate depth measurement could be done because of the strong agitation of the water surface caused by raindrops.

The flow velocity was measured using the salt-velocity gauge of Planchon et al. (2005). The device consisted of two pairs of conductivity probes, located in an upstream-downstream configuration, and spaced by 3 cm. A salt solution was added upstream from the first pair of electrodes and conductivity recordings were taken. The solution was supplemented with fluorescein to ensure the proper orientation of the device. The signals from the probes were used to solve a diffusion wave equation, allowing for the measurement of the flow velocity. For each location, the velocity value was the mean of ten readings.

The water depth and the flow velocity were measured at the nine same points at first. Considering the good homogeneity of the measured values, the number of measurement points per run was then reduced to three or four. The water flux was measured at the flume outlet by timing the partial filling of a tank, followed by the weighing of the tank.

The measurement of particle concentration was carried out at the flume outlet. The particles were collected in a sieve of 50 µm. A sieve was placed under the flow for one minute, and then replaced by another sieve. After the experimental run, the sieve contents were dried in an oven (90 ℃), and then weighed, allowing for the calculation of the particle flux. The particle concentration (in mg L^{-1}) was calculated as the ratio of particle flux and water flux.

During the design phase of the experiment, particle splash was measured by attaching a collector to the side of the experimental section. Almost no splashed material was collected. This means the particles entering the experimental section had only two possible fates: sedimenting on the flume bottom or reaching the flume outlet.

2.4 Experimental runs

The experimental runs consisted in two series. The first series, termed “oscillating-nozzle series”, paired a no-rainfall condition with an extremely high intensity condition. There was 3 replicates of such pair (plus a special run — see below). The second series, termed “drop-former series”, evaluated the effect of rainfall intensity from 0 to 55 mm h^{-1} using a total of 19 runs.

2.4.1 Oscillating-nozzle series

The first series of experimental runs made use of the oscillating-nozzle rainfall simulator, with a prescribed rainfall intensity of 175 mm h^{-1}. The rationale for running this series was that its extremely high rainfall intensity would increase the probability of interactions between raindrops and settling particles, hence maximizing the effects of the rain on particle sedimentation.

At the beginning of an experimental run, water depth, velocity and flux were measured. Then the no-rainfall condition was tested: the particle supply was launched for 7 min, with particle concentration being measured every minute at the outlet. After the end of the particle supply, water flux and particle concentration continued to be measured for three minutes. Subsequently, sedimented particles were manually cleaned from the flume bed, and the water flux measured. Then rainfall was initiated using the oscillating-nozzle rainfall simulator. The measurements were identical in their sequence and timing. Finally, the rainfall was stopped, and the water flux measured a last time.

This oscillating-nozzle series consisted of three experimental runs with paired condition: no-rainfall condition followed by rainfall condition, as described above. A fourth run is included: the rainfall condition (5 min long) was ran first and immediately followed by the no-rainfall condition (5 min long). In fact, this fourth run was initially considered to be flawed: the rainfall was stopped too early while the particle feeder was run for a longer duration. However, upon inspection, the data showed to be of interest, and so were included in the dataset.

2.4.2 Drop-former series

To assess the effect of rainfall intensity, a second series of experiments was carried out. The experiment setup was similar to the oscillating-nozzle series, except that the drop-former rainfall simulator was used, and that the runs were not carried out by pairs.

This series of lower rainfall intensities (compared to the first series) consisted of 19 experimental runs with a range of prescribed rainfall intensity: 3 runs with no rainfall (0 mm h^{-1}), and 2 runs at 10 mm h^{-1}, 3 runs at 15 mm h^{-1}, 2 runs at 25 mm h^{-1}, 7 runs at 35 mm h^{-1}, and 2 runs at 55 mm h^{-1}. The runs were not carried out in sequence of increasing rainfall intensity to avoid a bias. Initially, 2 to 3 runs per intensity were planned. Owing to the large differences in sediment concentration among the 35 mm h^{-1} runs, additional runs were carried out at this intensity.

2.5 Data analysis

At first, a qualitative assessment of tabulated values and graphs was carried out. Owing to the limited number of samples (that do not allow for asserting a normal distribution of residues), this primary analysis was complemented with non-parametric tests. The Wilcoxon test was carried out to compare two samples using R Core Team (2017). The Kruskall-Wallis test was used to check for the existence of differences among groups (Dinno, 2017). A significance level alpha of 5 % was considered. It must be noted that the tests are expected to have a low power, owing to the limited number of samples.

3 Results

3.1 Oscillating-nozzle series

3.1.1 Hydrodynamic conditions

Rainfall intensity varied between 157 and 192 mm h^{-1} (Table 1). Water depth was about 2.5 cm and water velocity about 9 cm s^{-1} (Table 1). Variations of water depth and water velocity were quite limited and not statistically significant ($P_{\text{water depth}} = 0.82$ and $P_{\text{water velocity}} = 0.50$).

Water flux at the outlet was around 74 L min^{-1} (Table 2). The water flux with rain was statistically higher than the water flux with the no rain condition ($P_{\text{water flux}} = 0.008$). The rainfall increased the water flux by about 0.8 L min^{-1} (i.e. by about 1 % of the total flux), which is consistent with the amount of water supplied by rain to the experimental section.

3.1.2 Particle concentration

Considering the first three runs, a similar evolution was observed with or without rain (Figure 2): the particle concentration at the outlet increased from the first to the second minute (i.e. from T = 0 to T = 2 min) and then reached a steady state. This steady state persisted up to the cut of the sediment supply (at T = 7 min). Then the particle concentration decreased sharply during the eighth minute, and became close to zero afterwards. This dynamics shows that the sediment supply has a direct control on the particle flux at the outlet.

Table 1: Rain intensity, water depth and water velocity for the oscillating-nozzle series.

Measurement condition		Rain intensity ($mm\,h^{-1}$) (n=4) Mean ± Std dev.	Water depth (cm) (n=9) Mean ± Std dev.	Water velocity ($cm\,s^{-1}$) (n=9) Mean ± Std dev.
Run 1	No rain	0	2.49 ± 0.09	9.2 ± 0.3
	Rain	157 ± 2	2.50 ± 0.09	9.0 ± 0.8
Run 2	No rain	0	2.55 ± 0.08	9.2 ± 0.7
	Rain	173 ± 5	2.54 ± 0.06	9.1 ± 0.5
Run 3	No rain	0	2.54 ± 0.06	9.3 ± 0.4
	Rain	192 ± 21	2.53 ± 0.07	9.3 ± 0.3
Run 4	No rain	0	ND	ND
	Rain	172 ± 2	2.50 ± 0.08	9.2 ± 0.5

n: number of samples

For a given run, there was always a clear difference in the concentration at steady-state between the rain and the no-rain conditions. And, among the runs, this difference was replicated: the particle concentration was about 15 $mg\,L^{-1}$ without rain, and about 10 $mg\,L^{-1}$ with rain, i.e. a 30 % decrease in particle concentration at the outlet.

The same behavior was observed in run 4: with rain and without rain, it took about one minute to reach the steady-state, and the particle concentration decreased after the cut of the sediment supply. During the rain application, the particle concentration at steady-state (12 $mg\,L^{-1}$) was higher than for the first three runs. After the rain was stopped, the particle concentration increased and stabilized at 15 $mg\,L^{-1}$.

The concentrations at steady-state are summarized in Figure 3. The concentration for the rain condition was significantly lower than the concentration for the no-rain condition (P = 0.015).

As supplementary observation, no sediment was found in the lateral pluviometers, ensuring that the particles were not splashed from the water flow into the air. Hence, all observations concur to a particle deposition hastened by the rain.

Table 2: Water flux at the outlet for the oscillating-nozzle series.

Measurement condition			Water flux ($L\,min^{-1}$) (n=6) Mean±Std dev.
Run 1	No rain	Before sediment supply	73.8 ± 0.4
		After sediment supply	73.7 ± 1.1
	Rain	Before rain	73.1 ± 0.9
		During rain	74.1 ± 0.7
		After rain	73.7 ± 0.6
Run 2	No rain	Before sediment supply	73.3 ± 0.8
		After sediment supply	73.7 ± 0.4
	Rain	Before rain	73.6 ± 0.4
		During rain	74.4 ± 0.3
		After rain	73.5 ± 0.7
Run 3	No rain	Before sediment supply	73.1 ± 0.3
		After sediment supply	73.0 ± 0.4
	Rain	Before rain	73.5 ± 0.4
		During rain	74.6 ± 0.5
		After rain	73.6 ± 0.7
Run 4	No rain	Before sediment supply	ND
		After sediment supply	ND
	Rain	Before rain	73.0 ± 0.3
		During rain	73.6 ± 0.7
		After rain	72.9 ± 0.5

ND: no data; n: number of samples

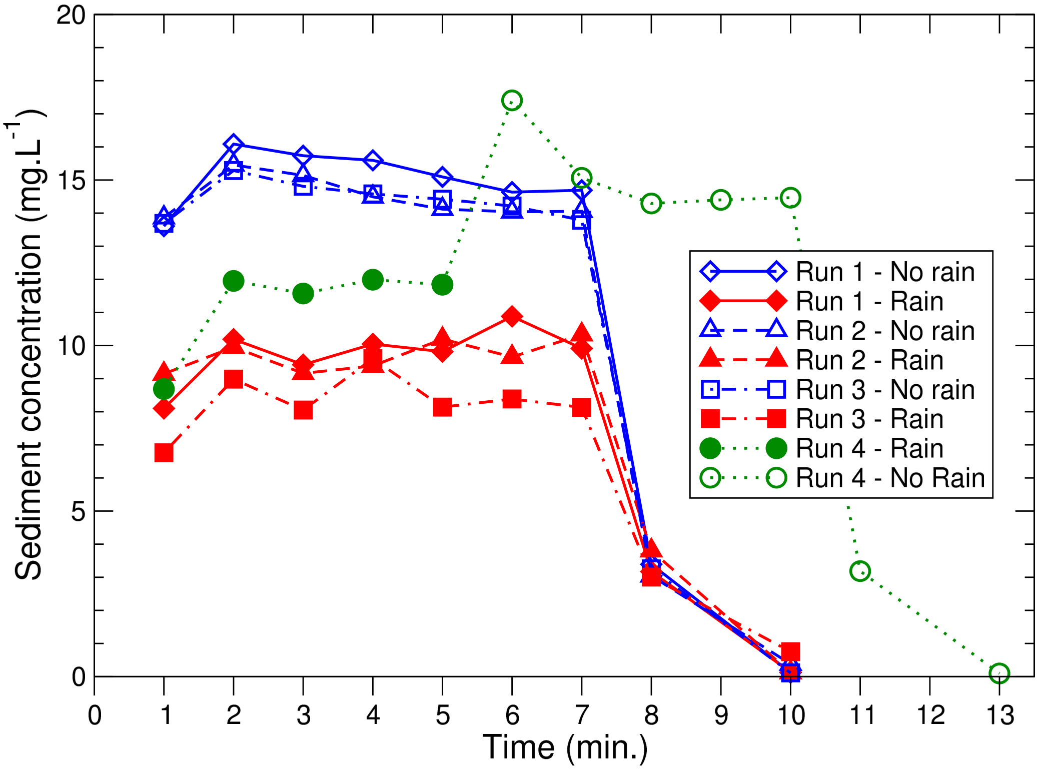

Figure 2: Time evolution of particle concentration at the outlet for the oscillating-nozzle series.
A value plotted at T = N min corresponds to the particle concentration measured from T = N − 1 min to T = N min.

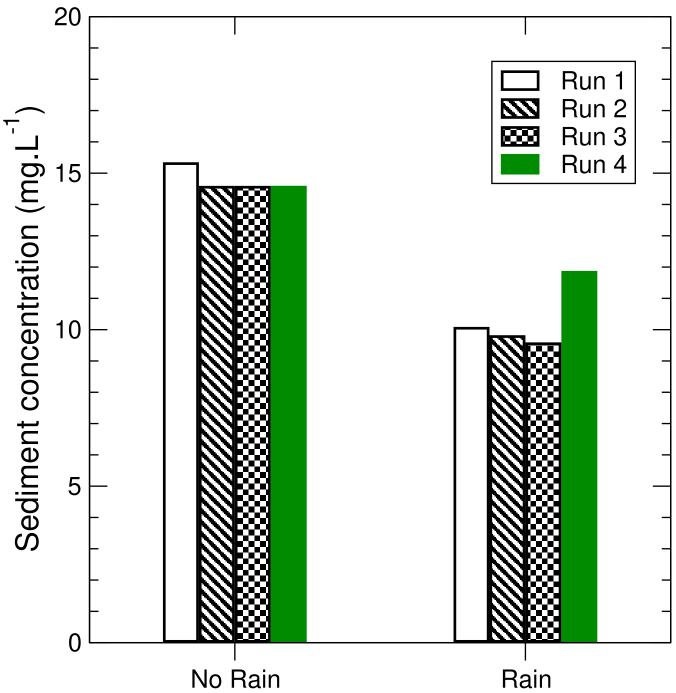

Figure 3: Mean particle concentration at steady-state at the outlet for the oscillating-nozzle series.
For the first three runs, values are considered for the range 2–7 min. For the fourth run, values are considered for the ranges 2–5 min (i.e. with rain) and 8–10 min (i.e. without rain).

3.2 Drop-former series

3.2.1 Hydrodynamic conditions

Actual rainfall intensities were generally close to the prescribed values (Table 3). As in the oscillating-nozzle series, water depths, velocities and fluxes had limited variations (Tables 3 and 4). Differences were not statistically significant ($P_{\text{water depth}} = 0.17$, $P_{\text{water velocity}} = 0.42$, and $P_{\text{water flux}} = 0.88$). The case "0 mm h^{-1} – run 2" had the highest mean velocity (9.7 m s^{-1}), but its water depth and flux were in the regular range. The lowest water flux was measured for the case "35 mm h^{-1} – run 1" (66 L min^{-1}), without obvious relation with its water depth and velocity.

For this drop-former series, the rainfall did not contribute significantly to the increase in the water flux at the outlet ($P_{\text{water flux}} = 0.39$). Indeed, at the maximal prescribed value of 55 mm h^{-1}, the contribution of the rainfall is expected to be of 0.2 L min^{-1}, which is three times lower than the average standard deviation (0.7 L min^{-1}) and 0.3 % of the total flux only.

3.2.2 Particle concentration

The flux of particles at the outlet (Figure 4) had a behavior similar to the one of the oscillating-nozzle series: an initial increase in the particle concentration from the first to the second minute, then a steady state, and, finally, a sharp decrease after the sediment supply was cut. For two runs (one at 0 mm h^{-1}, one at 60 mm h^{-1}), the sediment supply was continued for three extra minutes (because an operator forgot to stop the sediment feeder at the prescribed duration of 7 min). Except for their longer duration, these runs did not show a specific behavior.

Considering the steady states, the runs at 0 mm h^{-1} had the highest concentration. For the other rainfall intensities, the curves seemed intermingled. The runs at 35 mm h^{-1} had the largest range in concentration, especially with run 7 which showed the lowest concentration and a large shift between 3 and 4 min. For the runs at 10, 15, 25 and 55 mm h^{-1}, the range of variation was limited.

Summarizing the steady-state concentration with their mean values (Figure 5) gives a better view of the change in concentration with the rainfall

Table 3: Rain intensity, water depth and water velocity for the drop-former series.

Prescribed rain condition ($mm\,h^{-1}$)		Rain intensity ($mm\,h^{-1}$) Mean ± Std dev.	Water depth (cm) Mean ± Std dev.	Water velocity ($cm\,s^{-1}$) Mean ± Std dev.
0	Run 1	0	2.81 ± 0.04 n=4	8.2 ± 0.2 n=4
	Run 2	0	2.60 ± 0.02 n=3	9.7 ± 0.6 n=3
	Run 3	0	2.63 ± 0.04 n=3	8.2 ± 0.8 n=3
10	Run 1	9 ± 1 n=28	2.72 ± 0.12 n=9	8.2 ± 0.2 n=3
	Run 2	9 ± 1 n=28	2.72 ± 0.08 n=9	8.2 ± 0.2 n=3
15	Run 1	16 ± 2 n=28	2.69 ± 0.08 n=4	8.3 ± 0.1 n=4
	Run 2	16 ± 2 n=28	2.71 ± 0.04 n=4	8.2 ± 0.1 n=4
	Run 3	14 ± 2 n=28	2.52 ± 0.08 n=9	9.4 ± 0.1 n=3
25	Run 1	25 ± 3 n=27	2.64 ± 0.15 n=3	8.5 ± 0.4 n=3
	Run 2	26 ± 3 n=28	2.57 ± 0.41 n=9	8.5 ± 0.3 n=3
35	Run 1	37 ± 4 n=28	2.64 ± 0.08 n=9	8.6 ± 0.4 n=3
	Run 2	32 ± 3 n=28	2.68 ± 0.08 n=9	9.1 ± 1.7 n=3
	Run 3	35 ± 4 n=28	2.74 ± 0.11 n=4	8.2 ± 0.1 n=4
	Run 4	33 ± 7 n=8	2.71 ± 0.05 n=4	8.3 ± 0.2 n=4
	Run 5	34 ± 4 n=28	2.73 ± 0.07 n=4	8.1 ± 0.2 n=4
	Run 6	32 ± 4 n=28	2.81 ± 0.09 n=4	8.2 ± 0.2 n=4
	Run 7	35 ± 7 n=8	2.60 ± 0.02 n=3	9.1 ± 0.1 n=3
55	Run 1	52 ± 9 n=8	2.58 ± 0.04 n=9	9.3 ± 0.1 n=9
	Run 2	53 ± 12 n=8	2.51 ± 0.03 n=3	9.3 ± 0.1 n=3

n: number of samples.

Table 4: Water flux at the outlet for the drop-former series.

Measurement condition			Water flux
Prescribed rain ($mm\,h^{-1}$)			($L\,min^{-1}$) Mean ± Std dev.
0	Run 1	Before sediment supply	73.2 ± 0.6 n=6
		After sediment supply	73.2 ± 0.5 n=6
	Run 2	Before sediment supply	73.8 ± 0.6 n=6
		After sediment supply	73.9 ± 1.0 n=6
	Run 3	Before sediment supply	71.1 ± 0.5 n=6
		After sediment supply	70.7 ± 0.4 n=6
10	Run 1	Before rain	72.9 ± 0.7 n=6
		During rain	72.7 ± 0.5 n=6
		After rain	73.4 ± 0.4 n=6
	Run 2	Before rain	72.7 ± 0.4 n=6
		During rain	72.7 ± 0.7 n=6
		After rain	72.4 ± 1.2 n=6
15	Run 1	Before rain	72.2 ± 0.6 n=6
		During rain	71.8 ± 0.5 n=6
		After rain	72.6 ± 0.6 n=6
	Run 2	Before rain	73.0 ± 0.5 n=6
		During rain	73.1 ± 0.5 n=6
		After rain	73.2 ± 0.7 n=6
	Run 3	Before rain	71.3 ± 0.6 n=6
		During rain	71.4 ± 0.3 n=6
		After rain	71.3 ± 0.3 n=6
25	Run 1	Before rain	73.4 ± 0.5 n=6
		During rain	73.7 ± 0.5 n=6
		After rain	73.4 ± 0.4 n=6
	Run 2	Before rain	73.1 ± 0.7 n=6
		During rain	72.9 ± 1.1 n=5
		After rain	72.9 ± 0.5 n=6
35	Run 1	Before rain	65.6 ± 0.9 n=6
		During rain	66.4 ± 1.1 n=6
		After rain	65.9 ± 0.6 n=6
	Run 2	Before rain	73.0 ± 1.0 n=6
		During rain	73.2 ± 0.7 n=6
		After rain	73.0 ± 1.1 n=6
	Run 3	Before rain	73.6 ± 0.7 n=6
		During rain	74.0 ± 1.1 n=6
		After rain	73.2 ± 0.4 n=6
	Run 4	Before rain	73.5 ± 0.6 n=6
		During rain	73.6 ± 0.7 n=5
		After rain	73.5 ± 0.8 n=6
	Run 5	Before rain	71.5 ± 0.8 n=6
		During rain	71.4 ± 0.9 n=6
		After rain	71.7 ± 0.5 n=6
	Run 6	Before rain	71.8 ± 0.4 n=6
		During rain	71.7 ± 1.1 n=6
		After rain	71.7 ± 0.7 n=6
	Run 7	Before rain	71.4 ± 0.5 n=6
		During rain	73.5 ± 0.6 n=6
		After rain	73.8 ± 0.5 n=6
55	Run 1	Before rain	73.2 ± 0.5 n=6
		During rain	73.3 ± 0.8 n=6
		After rain	73.4 ± 0.4 n=5
	Run 2	Before rain	70.0 ± 3.6 n=6
		During rain	71.5 ± 0.8 n=6
		After rain	71.3 ± 0.6 n=6

n: number of samples.

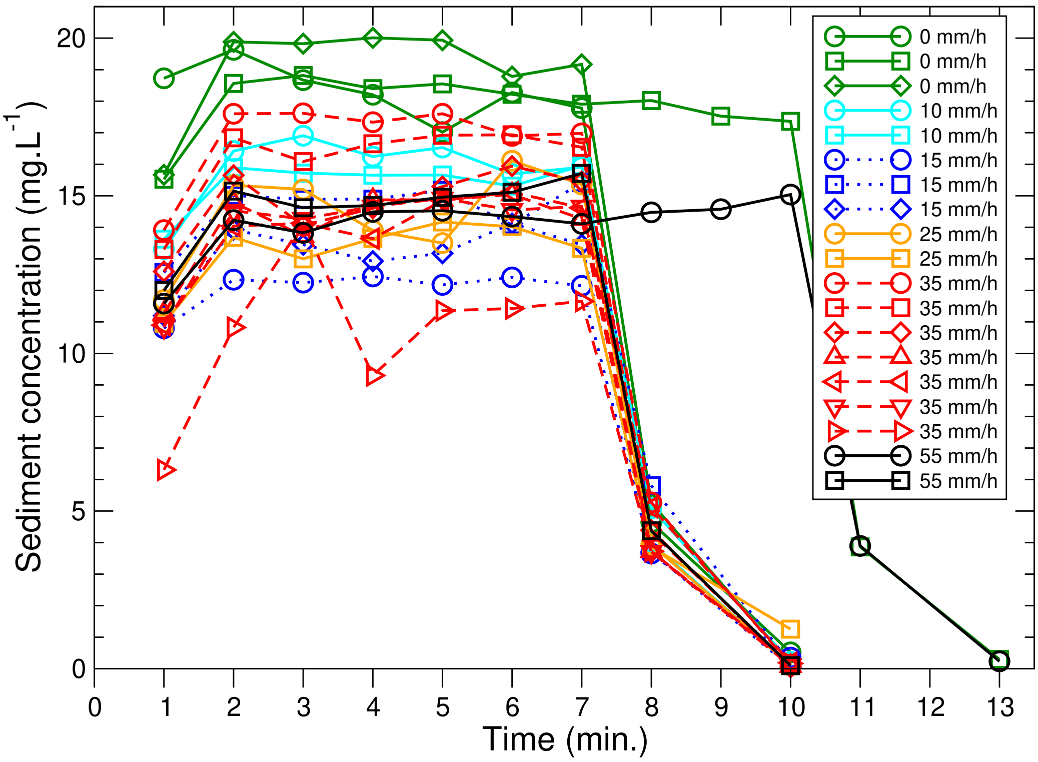

Figure 4: Time evolution of particle concentration at the outlet for the drop-former series.
The order of the cases in the legend is the same as in Tables 3 and 4.

intensity. The case 0 mm h^{-1} had the highest mean concentration (19 mg L^{-1}) and the case 15 mm h^{-1} had the lowest one (14 mg L^{-1}). When considering the experiments with rain compared to the experiments without rain, the Wilcoxon test showed that concentrations were significantly larger without rain (P = 0.004). However, the Kruskal-Wallis test did not show a significant difference in concentration among the rainfall intensities (P = 0.07).

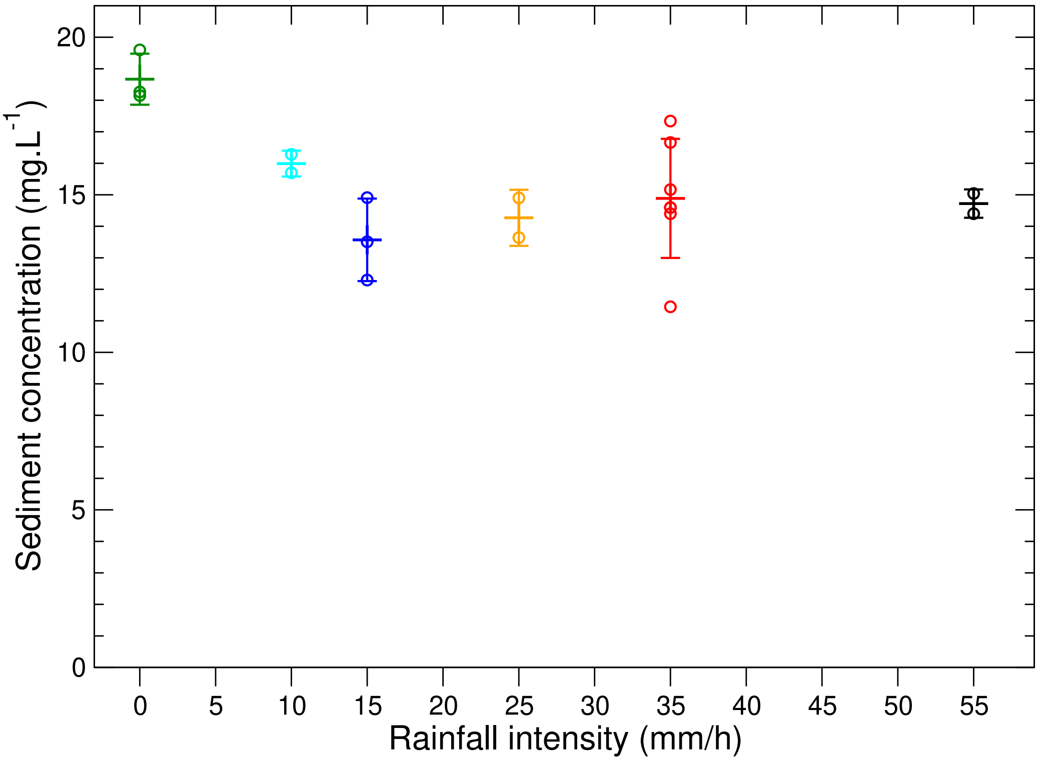

Figure 5: Particle concentration at steady-state at the outlet for the drop-former series.
Circles: mean concentration for each run. Bars: mean concentration and standard deviation for each rainfall intensity. For most of runs, the sediment concentration was calculated as the mean over the range 2–7 min. For the two longer runs, the range 2–10 min were used.

4 Discussion

4.1 Assessment of the experimental conditions

The experiments were carried out in a laboratory flume. They were designed to identify the effect of raindrops on particle sedimentation in sheet flow. Even if the experiments could look far from natural conditions, their features resemble sheet flow in interrill conditions: the water depth was only a few centimeters and the water velocity around one decimeter per second. While a smaller depth may have better mimic a typical sheet flow, the 2.5 cm depth was required to ensure that sedimented particles were not detached by the raindrop impacts. The conditions could be maintained through the whole experiment. The particle concentration was kept low to limit the interactions between particles. There was no significant particle splash, and, by design, particles were not detached after reaching the flume bottom. Hence, once delivered to the flow, the particles could have two fates only: being deposited at the bottom or reaching the outlet.

The highest rainfall intensity was around 175 mm h^{-1}. It was deemed to exacerbate the potential interactions between raindrops and particles. Such an intensity, while quite high, is not out of the natural range. Indeed, while these experiments supplied 30 mm of rainfall over a duration of about 10 min, the same amount of rainfall was observed over a single minute (WMO, 2020). However, we agree with Dunkerley (2020) that such high and constant rainfall intensity is quite unlike natural rainfall. Since this is the first study on the interaction between raindrops and settling particles, we believe that the use of rainfalls with such intensity is legitimate. Once this interaction characterized and understood, it will be necessary to investigate rainfalls with lower intensities and with time-varying intensities.

The contrast in concentration between the rain and no-rain conditions was larger for the first experimental series than for the second one. This could be related to the larger rainfall intensity of the first series (175 mm h^{-1}) compared to the second series (which as a maximum intensity of 55 mm h^{-1}). However, at this stage, and considering the insufficient understanding of the underlying processes and determinants, it would be preliminary to elaborate more on this: the contrast could be due not to differences in rainfall intensities but to differences in other rainfall properties — such as the raindrop sizes or the raindrop kinetic energies. While the first series had a higher rainfall intensity, it had a lower mean raindrop diameter (1.7 mm vs 3.0 mm), a lower specific kinetic energy ($7\,\mathrm{J\,m^{-2}\,mm^{-1}}$ vs $20\,\mathrm{J\,m^{-2}\,mm^{-1}}$), and was noticeably discontinuous. To reach a detailed explanation about the contrast between the two series will require a new experimental plan designed to separate the effect of the various rainfall properties.

4.2 Raindrop impacts foster particle sedimentation in sheet flow

For both the oscillating-nozzle and drop-former series, the particle concentration at the outlet was always the lowest when rainfall was applied.

This decrease in concentration could be due to the dilution of the particles by the supplementary water coming from the rain. However, while the rainfall increased the water flux at the outlet by up to one percent (in the oscillating-nozzle series), simultaneously, the particle concentration dropped by up to 30 %. This means that, overall, rainfall application decreased the particle flux to the outlet (from $1.1\,\mathrm{g\,min^{-1}}$ to $0.75\,\mathrm{g\,min^{-1}}$), leading to the conclusion that the supplementary water flux by the rainfall was not responsible for the observed results. So, the results indicate that the raindrop impacts fostered the particle sedimentation to the bottom of the flume. This conclusion was counter-intuitive to the authors of the experiments. Our initial rationale was that, by mixing and shaking the water flow (and this shaking was visually quite strong), the raindrop impacts would tend to prevent the sedimentation of particles, in a same way that mixing a bucket of muddy water slows down the particle settling. However, results were the exact opposite: raindrop impacts increased particle settling.

Of course, this conclusion is strictly valid for our experimental setup only, and this was the first experiment considering particle settling in sheet flow without detachment after sedimentation. Moreover, a limited range of conditions were tested. Rainfall intensity was the only variable; water depth, water velocity, water flux, particle size, particle density and particle flux were kept constant. Apart from the clear rain-no rain effect, there was no obvious relationship between rainfall intensity and particle concentration (drop-former series).

Being the first experiment to tackle the interaction between settling particles and raindrop in sheet flow, there is an obvious need for replication attempts. By underlining our lack of knowledge on the interactions between raindrops and particles in a flow, this calls for a broader evaluation of the effect of raindrop impacts on particle sedimentation.

Finally, the conclusion questions our current capability to consider settling velocities of particles in soil erosion models (De Roo et al., 1996; Morgan et al., 1998; Hairsine et al., 2002; Wainwright et al., 2008), especially when settling velocities are adjusted to better fit measurements at the outlet (Tromp-van Meerveld et al., 2008; Jomaa et al., 2010). It is recognized that the calibration of numerous parameters leads to equifinality, limiting the confidence in the simulation outputs (Beven, 2008). Adding more constraints on model parameters will decrease the degree of freedom of the models, and help in enhancing confidence in modeling efforts (Kirstetter et al., 2016).

4.3 Mechanisms that could increase the settling velocity

The conclusion that raindrop impacts increase settling velocity raises questions about the underlying mechanisms. If, obviously, it was not the result of a simple mixing as in a muddy bucket, two other potential mechanisms are proposed.

Raindrops impacting a sheet flow do not only cause a shaking of the flow and a supplementary water flux. They also add a vertical momentum. Conceptually, the vertical movement of particles can be separated into gravity-induced settling (i.e. the settling observed in still water) and an additional motion caused by the raindrop impacts. Individual raindrops might be pushing downward the volume of water underneath, and the incorporated particles. Of course, this finally gets balanced with upward movements, and goes along with lateral movements of both water and particles. It is hypothesized that raindrops do not cause a simple mixing/shaking as done by hand in a muddy bucket, but that a more complex interaction occurs.

Because the probability of a raindrop-particle interaction increases with the number of raindrops (Nouhou Bako et al., 2017), such an interaction should depend on the rainfall intensity. Since no such a dependency was observed in the presented results, it could be argued that this mechanism should be discarded. It could also be argued that it is compensated by another (and unknown) phenomenon. However, considering the huge lack of knowledge on this subject, we will refrain from further consideration. We simply call for further investigations. These investigations could advantageously make use of the recent advances in computational fluid dynamics

(Nouhou Bako et al., 2016; Nouhou-Bako et al., 2019).

The experiments without rainfall had a Reynolds number of 2250. When considering that the transition between laminar and turbulent regimes are at a Reynolds number of 2500, it could be argued that the application of rainfall caused the flow to go from laminar to turbulent. If the turbulent regime was already in place at the lowest rainfall intensity ($10\,\mathrm{mm\,h^{-1}}$), its effect would also be present at higher rainfall intensities (i.e. from $15\,\mathrm{mm\,h^{-1}}$ to $55\,\mathrm{mm\,h^{-1}}$). This could explain that the sediment concentration kept statistically the same for the $10\,\mathrm{mm\,h^{-1}}$ to $55\,\mathrm{mm\,h^{-1}}$ intensities.

Many authors have made experimental and numerical studies about how the settling velocity of a particle is modified in the turbulent regime (Gore and Crowe, 1990; Mei et al., 1991; Wang and Maxey, 1993; Warnica et al., 1995; Brucato et al., 1998; Bagchi and Balachandar, 2003). These studies analyzed the modification of the particle drag coefficient when the flow regime changed from laminar to turbulent, and their results are reviewed in Bagchi and Balachandar (2003). In summary, these results can be classified into three categories:

1. Some studies have observed a decrease of the settling velocity when the regime goes from laminar to turbulent (Uhlherr and Sinclair, 1970; Zarin and Nicholls, 1971; Brucato et al., 1998). This decrease may be due to the non-linear dependency of the drag coefficient with the settling velocity. When the turbulence intensity increases, the drag coefficient also increases, leading to a decrease of the settling velocity. This effect is significant for particles having sizes larger than the Kolmogorov scale, the turbulent energy being dissipated by small vortex structures.
2. Other studies like Rudolff and Bachalo (1988) and Gore and Crowe (1990) have observed an increase of the settling velocity in the turbulent regime. These authors explain the augmentation of the settling velocity by the fact that particles have preferential trajectories in turbulent flow. Particles “prefer” regions of downward flow compared to regions of upward flow. This effect is dominant for particles smaller or of the order of the Kolmogorov scale.
3. For some studies like Warnica et al. (1995) and Bagchi and Balachandar (2003), the turbulence has no significant effect on the settling velocity of particles. This velocity remains the same regardless the nature of the flow.

Our results are in agreement with the observations of the second category of studies: their results and those presented in this article show an increase of the settling velocity of particles when moving to a turbulent regime.

During the experiments, no turbulence measurement was carried out, and so, the Kolmogorov scale could not be estimated. Indeed, turbulence measurements as well as the Kolmogorov scale are unheard in soil erosion studies. The cited studies come from the fluid mechanics community. There is a large stretch between our knowledge and practices in water soil erosion and the knowledge and practices in fluid mechanics. The experimental conditions and setup of the cited studies are quite different from what we are used to, and sheet flow is not even a concept in fluid mechanics. Hence, the present study calls for a collaboration with the fluid mechanics community. We believe that bridging the gap between our communities could foster knowledge development about the settling of particles in sheet flow, and, more generally about soil erosion processes by water.

5 Conclusions

A laboratory flume experiment under simulated rainfall was specifically designed to address the effect of raindrop impacts on the settling of particles in sheet flow. Depth and velocity were close to conditions observed in sheet flow. The flow was supplied with 100–200 µm particles which concentration was measured at the outlet.

A first set of experiments, using an oscillating-nozzle rainfall simulator, compared a no rainfall condition with a high rainfall intensity condition (175 mm h^{-1}). It showed that the raindrop impacts decreased the particle concentration at the outlet by about 30 percent. Using a drop-former rainfall simulator, this effect was confirmed by a second set of lower rainfall intensity experiments (0, 10, 15, 25, 35, 55 mm h^{-1}), also no obvious relationship was found with the rainfall intensity. The study concluded that the raindrop impacts increase particle sedimentation in sheet flow. This questions the current practice of adjusting the particle settling velocities to better fit model outputs at the outlet.

While the underlying mechanism could not be determined, it could be related to the momentum of the raindrops, to the turbulence caused by the raindrops into the flow, or to the combination of both. Further studies need to be carried out, including replication attempts. The use of computational fluid dynamics and collaboration with the fluid mechanics community are encouraged.

References

Bagchi, P. and Balachandar, S. (2003). Effect of turbulence on the drag and lift of a particle. *Physics of Fluids*, 15(11):3496–3513, DOI: 10.1063/1.1616031.

Beven, K. (2008). On doing better hydrological science. *Hydrological processes*, 22(17):3549–3553, DOI: 10.1002/hyp.7108.

Brucato, A., Grisafi, F., and Montante, G. (1998). Particle drag coefficients in turbulent fluids. *Chemical Engineering Science*, 53(18):3295–3314, DOI: 10.1016/S0009-2509(98)00114-6.

Cheng, N. S. (1997). Simplified settling velocity formula for sediment particle. *Journal of Hydraulic Engineering*, 123(2):149–152, DOI: 10.1061/(ASCE)0733-9429(1997)123:2(149).

Cottenot, L., Courtemanche, P., Nouhou-Bako, A., and Darboux, F. (2021). A rainfall simulator using porous pipes as drop former. *Catena*, 200:105101, DOI: 10.1016/j.catena.2020.105101.

De Roo, A. P. J., Wesseling, C. G., and Ritsema, C. J. (1996). LISEM: a single-event, physically based hydrological and soil erosion model for drainage basins. I: Theory, input and output. *Hydrological processes*, 10(8):1107–1117, DOI: 10.1002/(SICI)1099-1085(199608)10:8<1107::AID-HYP415>3.0.CO;2-4.

Dinno, A. (2017). *dunn.test: Dunn's test of multiple comparisons using rank sums*, https://CRAN.R-project.org/package=dunn.test. R package version 1.3.5.

Dunkerley, D. (2020). Rainfall intensity in geomorphology: Challenges and opportunities. *Progress in Physical Geography: Earth and Environment*, page 030913332096789, DOI: 10.1177/0309133320967893.

Foster, G. R., Eppert, F. P., and Meyer, L. D. (1979). A programmable rainfall simulator for field plots. In *Proceedings of the rainfall simulator workshop. Tucson, Arizona. March 7–9, 1979*, pages 45–59, Sidney, Montana. Agricultural Reviews and Manuals, ARM-W-10. United States Department of Agriculture - Science and Education Administration, Oakland, CA, https://books.google.fr/books?id=-DlDble2vPsC&ots=EfE-wj43Di.

Ghadiri, H. and Payne, D. (1988). The formation and characteristics of splash following raindrop impact on soil. *Journal of Soil Science*, 39(4):563–575, DOI: 10.1111/j.1365-2389.1988.tb01240.x.

Gore, R. A. and Crowe, C. T. (1990). Discussion of "particle drag in a dilute turbulent two-phase suspension flow". *International Journal of Multiphase Flow*, 16(2):359–361, DOI: 10.1016/0301-9322(90)90065-Q.

Hairsine, P. B., Beuselinck, L., and Sander, G. C. (2002). Sediment transport through an area of net deposition. *Water Resources Research*, 38(6):22–1–22–7, DOI: 10.1029/2001wr000265.

Huang, C. (1995). Empirical analysis of slope and runoff for sediment delivery from interrill areas. *Soil Science Society of America Journal*, 59(4):982–990, DOI: 10.2136/sssaj1995.03615995005900040004x.

Jomaa, S., Barry, D. A., Brovelli, A., Sander, G. C., Parlange, J.-Y., Heng, B. C. P., and Tromp-van Meerveld, H. J. (2010). Effect of raindrop splash and transversal width on soil erosion: laboratory flume experiments and analysis with the Hairsine-Rose model. *Journal of Hydrology*, 395(1–2):117–132, DOI: 10.1016/j.jhydrol.2010.10.021.

Kinnell, P. I. A. (1990). The mechanics of raindrop-induced flow transport. *Australian Journal of Soil Research*, 28(4):497–516, DOI: 10.1071/SR9900497.

Kinnell, P. I. A. (1991). The effect of flow depth on sediment transport induced by raindrops impacting shallow flows. *Transactions of the ASAE*, 34(1):161–168, DOI: 10.13031/2013.31639.

Kinnell, P. I. A. (2005). Raindrop-impact-induced erosion processes and prediction: a review. *Hydrological Processes*, 19(14):2815–2844, DOI: 10.1002/hyp.5788.

Kinnell, P. I. A. (2011). Raindrop-induced saltation and the enrichment of sediment discharged from sheet and interrill erosion areas. *Hydrological Processes*, 26(10):1449–1456, DOI: 10.1002/hyp.8270.

Kinnell, P. I. A. (2021). Technical note: Detachment and transport limiting systems operate simultaneously in raindrop driven erosion. *Catena*, 197:104971, DOI: 10.1016/j.catena.2020.104971.

Kirstetter, G., Hu, J., Delestre, O., Darboux, F., Lagrée, P.-Y., Popinet, S., Fullana, J. M., and Josserand, C. (2016). Modeling rain-driven overland flow: Empirical versus analytical friction terms in the shallow water approximation. *Journal of hydrology*, 536:1–9, DOI: 10.1016/j.jhydrol.2016.02.022, https://hal.archives-ouvertes.fr/hal-01191401.

Kuhn, N. J. and Bryan, R. B. (2004). Drying, soil surface condition and interrill erosion on two Ontario soils. *Catena*, 57(2):113–133, DOI: 10.1016/j.catena.2003.11.001.

Leguédois, S., Planchon, O., Legout, C., and Le Bissonnais, Y. (2005). Splash projection distance for aggregated soils. theory and experiment. *Soil Science Society of America Journal*, 69(1):30–37, DOI: 10.2136/sssaj2005.0030.

Mei, R., Adrian, R. J., and Hanratty, T. J. (1991). Particle dispersion in isotropic turbulence under Stokes drag and Basset force with gravitational settling. *Journal of Fluid Mechanics*, 225:481–495, DOI: 10.1017/S0022112091002136.

Morgan, R. P. C., Quinton, J. N., Smith, R. E., Govers, G., Poesen, J. W. A., Auerswald, K., Chisci, G., Torri, D., and Styczen, M. E. (1998). The European Soil Erosion Model (EUROSEM): a dynamic approach for predicting sediment transport from fields and small catchments. *Earth surface processes and landforms*, 23:527–544, DOI: 10.1002/(SICI)1096-9837(199806)23:6<527::AID-ESP868>3.0.CO;2-5.

Moss, A. J. (1988). Effects of flow-velocity variation on rain-driven transportation and the role of rain impact in the movement of solids. *Australian Journal of Soil Research*, 26(3):443–450, DOI: 10.1071/SR9880443.

Moss, A. J. and Green, P. (1983). Movement of solids in air and water by raindrop impact. effects of drop-size and water-depth variations. *Australian Journal of Soil Research*, 21(3):257–269, DOI: 10.1071/SR9830257.

Nord, G. and Esteves, M. (2005). PSEM_2D: a physically based model of erosion processes at the plot scale. *Water Resources Research*, 41(8), DOI: 10.1029/2004WR003690.

Nouhou Bako, A., Darboux, F., James, F., Josserand, C., and Lucas, C. (2016). Pressure and shear stress caused by raindrop impact at the soil surface: Scaling laws depending on the water depth. *Earth surface processes and landforms*, 41(9):1199–1210, DOI: 10.1002/esp.3894.

Nouhou Bako, A., Darboux, F., James, F., and Lucas, C. (2017). Raindrop interaction in interrill erosion for steady rainfalls: A probabilistic approach. *Water Resources Research*, 53(5):4361–4375, DOI: 10.1002/2017WR020568.

Nouhou-Bako, A., Darboux, F., James, F., and Lucas, C. (2019). Rainfall erosivity in interrill areas: Insights about the choice of an erosive factor. *Catena*, 180:24–31, DOI: 10.1016/j.catena.2019.02.025.

Planchon, O., Silvera, N., Gimenez, R., Favis-Mortlock, D., Wainwright, J., Le Bissonnais, Y., and Govers, G. (2005). An automated salt-tracing gauge for flow-velocity measurement. *Earth Surface Processes and Landforms*, 30(7):833–844, DOI: 10.1002/esp.1194.

Proffitt, A. P. B. and Rose, C. W. (1991). Soil erosion processes — 1. The relative importance of rainfall detachment and runoff entrainment. *Australian Journal of Soil Research*, 29(5):671–683, DOI: 10.1071/SR9910671.

Proffitt, A. P. B., Rose, C. W., and Hairsine, P. B. (1991). Rainfall detachment and deposition: experiments with low slopes and significant water depths. *Soil Science Society of America Journal*, 55(2):325–332, DOI: 10.2136/sssaj1991.03615995005500020004x.

R Core Team (2017). *R: a language and environment for statistical computing*. R Foundation for Statistical Computing, Vienna, Austria, https://www.R-project.org/. Version 3.3.3.

Rudolff, R. C. and Bachalo, W. D. (1988). Measurement of droplet drag coefficients in polydispersed turbulent flow field. In *26th Aerospace Sciences Meeting, Reno, NV, January 11-14.* American Institute of Aeronautics and Astronautics, DOI: 10.2514/6.1988-235.

Römkens, M. J. M., Helming, K., and Prasad, S. N. (2002). Soil erosion under different rainfall intensities, surface roughness, and soil water regimes. *Catena*, 46(2–3):103–123, DOI: 10.1016/S0341-8162(01)00161-8.

Tromp-van Meerveld, H. J., Parlange, J.-Y., Barry, D. A., Tromp, M. F., Sander, G. C., Walter, M. T., and Parlange, M. B. (2008). Influence of sediment settling velocity on mechanistic soil erosion modeling. *Water Resources Research*, 44(6):W06401, DOI: doi:10.1029/2007WR006361.

Uhlherr, P. H. T. and Sinclair, C. G. (1970). The effect of free stream turbulence on the drag coefficients of spheres. In *Proceedings of Chemeca'70*, volume 1, pages 1–13, Butterworths. Melbourne. Australia.

Wainwright, J., Parsons, A. J., Müller, E. N., Brazier, R. E., Powel, D. M., and Fenti, B. (2008). A transport-distance approach to scaling erosion rates: I. background and model development. *Earth surface processes and landforms*, 33(5):813–826, DOI: 10.1002/esp.1624.

Wang, L.-P. and Maxey, M. R. (1993). Settling velocity and concentration distribution of heavy particles in homogeneous isotropic turbulence. *Journal of Fluid Mechanics*, 256:27–68, DOI: 10.1017/S0022112093002708.

Warnica, W. D., Renksizbulut, M., and Strong, A. B. (1995). Drag coefficients of spherical liquid droplets. part 2: Turbulent gaseous fields. *Experiments in Fluids*, 18(4):265–276, DOI: 10.1007/BF00195097.

WMO (2020). World weather and climate extremes archive. World Meteorological Organization. Accessed on 12 August 2020. https://wmo.asu.edu.

Zarin, N. A. and Nicholls, J. A. (1971). Sphere drag in solid rockets — non-continuum and turbulence effects. *Combustion Science and Technology*, 3(6):273–285, DOI: 10.1080/00102207108952295.

Zhang, X. C. (2019). Determining and modeling dominant processes of interrill soil erosion. *Water Resources Research*, 55(1):4–20, DOI: 10.1029/2018wr023217.